Dynamics analysis of a mobile crane with taking into account the hanged load eccentricity

Andrzej Urbaś, Krzysztof Augustynek, Jacek Stadnicki

Department of Mechanical Engineering Fundamentals
University of Bielsko-Biala
Willowa 2, 43-309, Poland
(aurbas,kaugustynek,jstadnicki)@ath.bielsko.pl

ABSTRACT

The method of modelling a load and a rope sling system has a significant impact not only on its dynamics but also on the dynamics of the crane. The literature is rather dominated by simplified models, in which the load is treated as a lumped mass, less frequently as a rigid body, and hanged on one rope, which end is fixed to the centroid of the load. The model of a mobile crane with the load as a rigid body hanged eccentrically on a rope sling system is presented and discussed in the paper. The influence of the eccentricity on the load positioning correctness is examined.

Keywords: dynamics, mobile crane, load eccentricity, drive flexibility, positioning indicator.

1 INTRODUCTION

Cranes are the most common handling devices. An important aspect of the crane's operation is the control of the position of the load during the manoeuvre and immediately after its completion. It is important to know the factors that affect the load behaviour and to predict the load's response due to these factors. One of the most essential components which can have an influence on the load movement is its eccentric suspension. This means that the attachment point or the centre of the block load is shifted relative to the position of the centre of mass of the load and its main axes of inertia. Such suspension can lead to additional load swings and twists. Gao et al. in [1] show a dynamics model of a bridge crane carrying heterogeneous loads hanged on two ropes. The negative impact of the eccentricity on the load movement is compensated by the model based control system proposed by the authors. The control strategy is verified experimentally. Oscillations of the load in the form of the slender-payload or log are analysed in [2-5]. In mathematical model proposed in [2] the load is hanged on two cables to the trolley and only three generalized coordinates are taken into account (angle of rotary column, swing angles of the load). More complicated model is presented in [3-5] where the load is hanged using double-pendulum system. The aforementioned papers focus only on the proper selection of the load control strategy to minimize its oscillations and the effect of the load eccentricity is not analysed. Double-pendulum dynamics due to distributed-mass payloads is investigated also in [6]. Kacalak et al. in [7] examine the impact of the sequence of work movements and the range of applied kinematic inputs on the accuracy of load positioning. In this case the load is modelled as a box and the load eccentricity is not taken into account. In [8] authors study three different variants of a load: lumped mass on one hook-sling, sphere on one hook-sling, and box on four hook-slings. The results obtained prove that the simplifications used in modelling the load have a huge impact on its dynamics. In conclusion, it can be stated that there is a small number of papers dealing with the load eccentricity effect on the carried load the dynamics.

The aim of this work is to examine how the change of direction and the value of eccentricity affect the movement of the load in the form of a block. The paper is organized as follows. In section 2 dynamics model of the crane with an eccentrically suspended load is given. Section 3 presents data assumed and numerical simulations results. In this section additional indicators are defined

for evaluating positioning accuracy. The paper ends with summary.

2 MATHEMATICAL MODEL OF THE SYSTEM

The authors propose the mathematical model of a crane with a rigid body load, hanged eccentrically on a rope sling system (Fig. 1). The proposed model of the crane includes: crane suspension subsystem b, supporting structure c_m (consists of a rotary column, two boom sections and a telescopic boom section) and two load lifting subsystems $c_{a,\alpha}\big|_{\alpha\in\{1,2\}}$ (refer to hydraulic cylinders). The carried load is modelled as block hanged eccentrically on the rope sling system ($e_\alpha\big|_{\alpha\in\{x,y,x,y\}} \in \{0, 0.1, 0.2\}\,\mathrm{m}$).

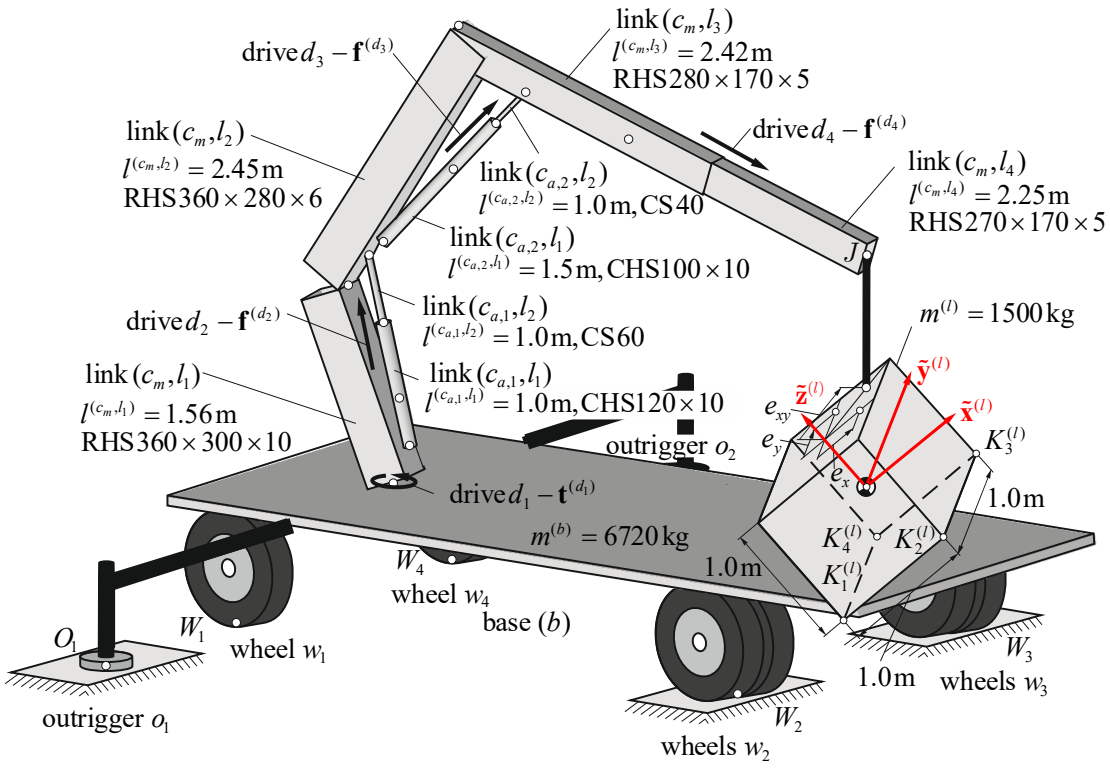

Figure 1. *Model of the crane and load*

The crane movement cycle is realized by rigid or flexible drives and divided into five phases, i.e. load lowering ($\mathbf{f}^{(d_3)}$), crane rotating ($\mathbf{t}^{(d_1)}$), load telescoping ($\mathbf{f}^{(d_4)}$), load lifting ($\mathbf{f}^{(d_2)}$) and load free swinging.

2.1 Kinematics of the crane and load

In order to describe the kinematics of the system, the formalism of the joint coordinates and the Denavit-Hartenberg is used (Fig.2).

The motion of the crane and load can be expressed by the following generalized coordinates vector

$$\mathbf{q} = \left[\, \mathbf{q}^{(c)^T} \;\middle|\; \mathbf{q}^{(l)^T} \,\right] = \left[\, \mathbf{q}^{(b)^T} \quad \overline{\mathbf{q}}^{(c_m)^T} \quad \overline{\mathbf{q}}^{(c_{a,1})^T} \quad \overline{\mathbf{q}}^{(c_{a,2})^T} \;\middle|\; \mathbf{q}^{(l)^T} \,\right]^T, \tag{1}$$

where: $\mathbf{q}^{(c)}, \mathbf{q}^{(l)}$ define the motion of the crane and the load, respectively.

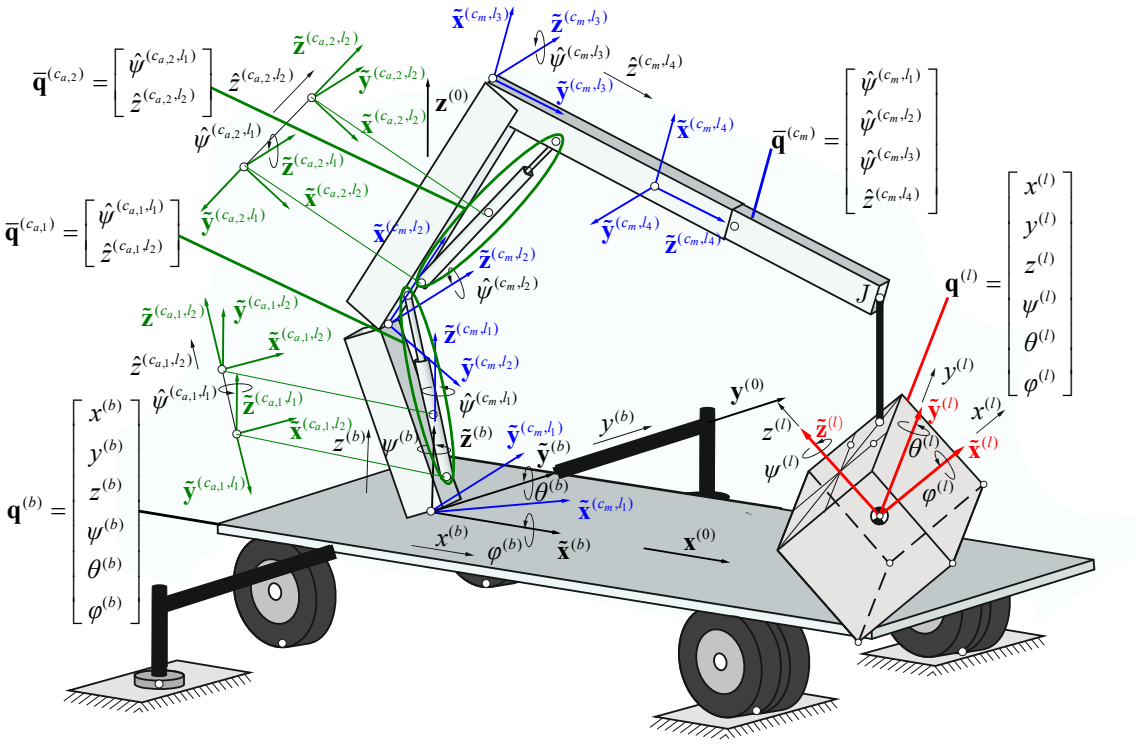

Figure 2. *Generalized coordinates in its proper coordinate systems*

2.2 Dynamics of the crane and load

The equations of motion are derived using the Lagrange equations of the second kind. These equations are supplemented by the constraint equations formulated in the cut-joints both for rigid and flexible drives.

They can be written as follows:

- if drives are rigid

$$\begin{bmatrix} \mathbf{M}^{(c)} & \mathbf{0} & \mathbf{C}^{(j)^T} & \mathbf{C}^{(d)^T} \\ \mathbf{0} & \mathbf{M}^{(l)} & \mathbf{0} & \mathbf{0} \\ \mathbf{C}^{(j)} & \mathbf{0} & \mathbf{0} & \mathbf{0} \\ \mathbf{C}^{(d)} & \mathbf{0} & \mathbf{0} & \mathbf{0} \end{bmatrix} \begin{bmatrix} \ddot{\mathbf{q}}^{(c)} \\ \ddot{\mathbf{q}}^{(l)} \\ \mathbf{f}^{(j)} \\ \mathbf{f}^{(d)} \end{bmatrix} = \begin{bmatrix} \mathbf{f}^{(c)} \\ \mathbf{f}^{(l)} \\ \mathbf{d}^{(j)} \\ \mathbf{d}^{(d)} \end{bmatrix}, \tag{2.1}$$

- if drives are flexible

$$\begin{bmatrix} \mathbf{M}^{(c)} & \mathbf{0} & \mathbf{C}^{(j)^T} \\ \mathbf{0} & \mathbf{M}^{(l)} & \mathbf{0} \\ \mathbf{C}^{(j)} & \mathbf{0} & \mathbf{0} \end{bmatrix} \begin{bmatrix} \ddot{\mathbf{q}}^{(c)} \\ \ddot{\mathbf{q}}^{(l)} \\ \mathbf{f}^{(j)} \end{bmatrix} = \begin{bmatrix} \mathbf{f}^{(c)} \\ \mathbf{f}^{(l)} \\ \mathbf{d}^{(j)} \end{bmatrix}, \tag{2.2}$$

where:

$\mathbf{M}^{(c)}$, $\mathbf{M}^{(l)}$ are the mass matrices of the crane and load,

$\mathbf{C}^{(j)}$, $\mathbf{C}^{(d)}$ are the constraint matrices related to the cut-joints and drives,

$\mathbf{f}^{(j)}$ is the vector of unknown reaction forces in the cut-joints,

$\mathbf{f}^{(d)}$ is the vector of the unknown driving torque and forces,

$\mathbf{f}^{(c)}$, $\mathbf{f}^{(l)}$ are the vectors of the right side of the dynamics equations,

$$\mathbf{f}^{(c)} = \begin{cases} -\mathbf{e}^{(c)} - \mathbf{g}^{(c)} - \mathbf{s}^{(s)} - \mathbf{s}^{(r,c_m)} & \text{if rigid drives,} \\ -\mathbf{e}^{(c)} - \mathbf{g}^{(c)} - \mathbf{s}^{(s)} - \mathbf{s}^{(d)} - \mathbf{s}^{(r,c_m)} & \text{if flexible drives,} \end{cases}$$

$$\mathbf{f}^{(l)} = -\mathbf{e}^{(l)} - \mathbf{g}^{(l)} - \mathbf{s}^{(r,l)}$$

$\mathbf{e}^{(c)}$, $\mathbf{e}^{(l)}$ are the vectors of the Coriolis, gyroscopic, and centrifugal forces,

$\mathbf{g}^{(c)}$, $\mathbf{g}^{(l)}$ are the vectors of the gravity forces,

$\mathbf{s}^{(s)}$ is the vector of the spring and damping forces formulated to the wheels and outriggers,

$\mathbf{s}^{(d)}$ is the vector of the spring and damping torque and forces formulated to the flexible drives,

$\mathbf{s}^{(r,c_m)}$, $\mathbf{s}^{(r,l)}$ are the vectors of the spring and damping force(s) formulated to the rope(s),

$\mathbf{d}^{(j)}$, $\mathbf{d}^{(d)}$ are the vectors of the right side of the constraints.

3 NUMERICAL CALCULATIONS

The crane input is divided into five phases (Fig. 3).

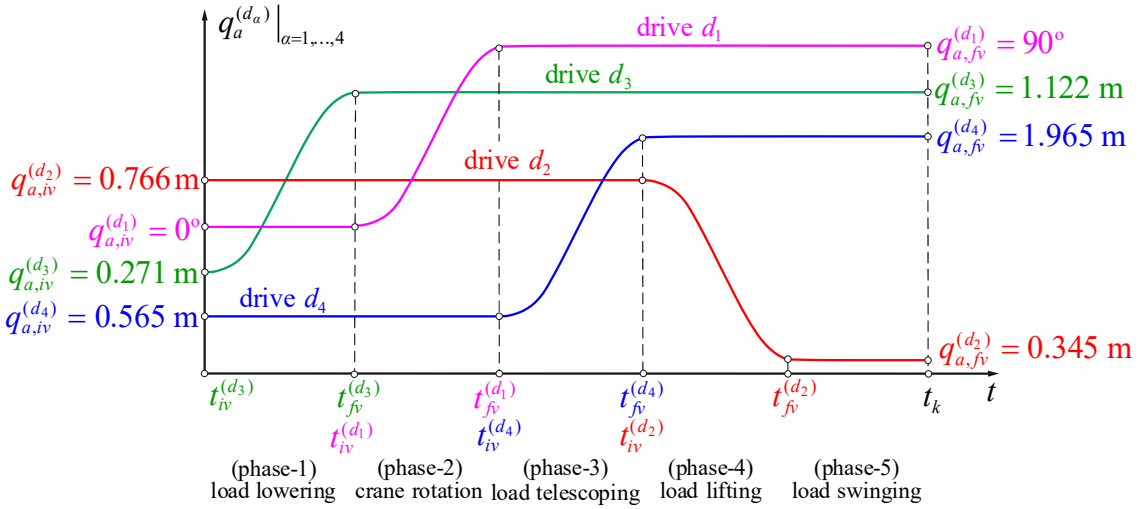

Figure 3. *Assumed input courses of drives of the crane.*

The fourth order Runge–Kutta method with a constant step size equal to 10^{-4} s is used to integrate the dynamics equations.

Figs 4 presents the trajectories of $K_i^{(l)}|_{i\in\{1,\ldots,4\}}$ points of the block load in $\mathbf{x}^{(0)}\mathbf{y}^{(0)}$ plane in case when the load is hanged at centroid ($e_\alpha|_{\alpha\in\{x,y,xy\}} = 0$) for rigid and flexible drives.

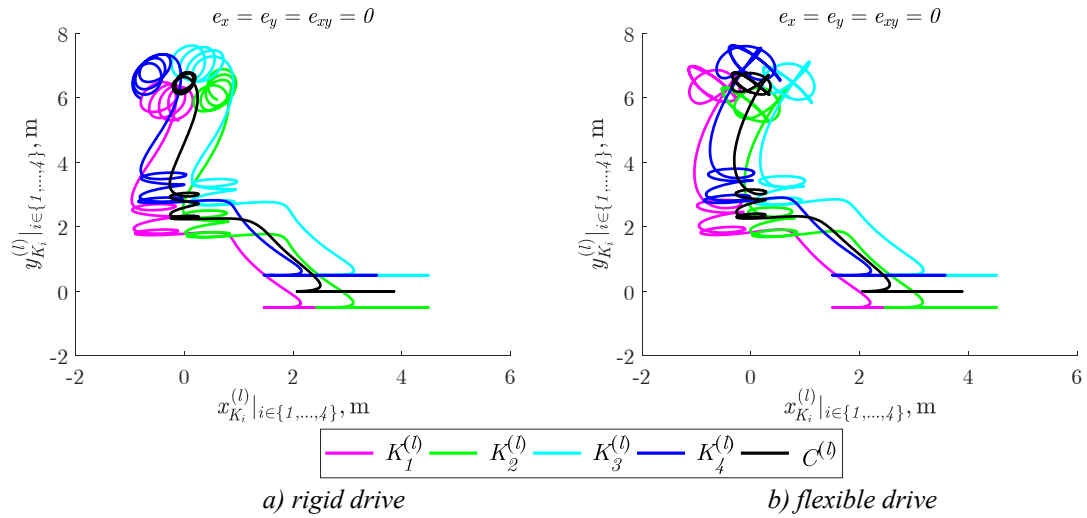

a) rigid drive *b) flexible drive*

Figure 4. *Trajectories of* $K_i^{(l)}|_{i\in\{1,\ldots,4\}}$ *points of the load hanged centrally*

Fig. 5 shows the trajectories of $K_i^{(l)}|_{i\in\{1,\ldots,4\}}$ points of the block load in $\mathbf{x}^{(0)}\mathbf{y}^{(0)}$ plane when the load is hanged eccentrically along $\tilde{\mathbf{x}}^{(l)}$ axis direction. The eccentricity is assumed as $e_x = 0.1$ or 0.2 m.

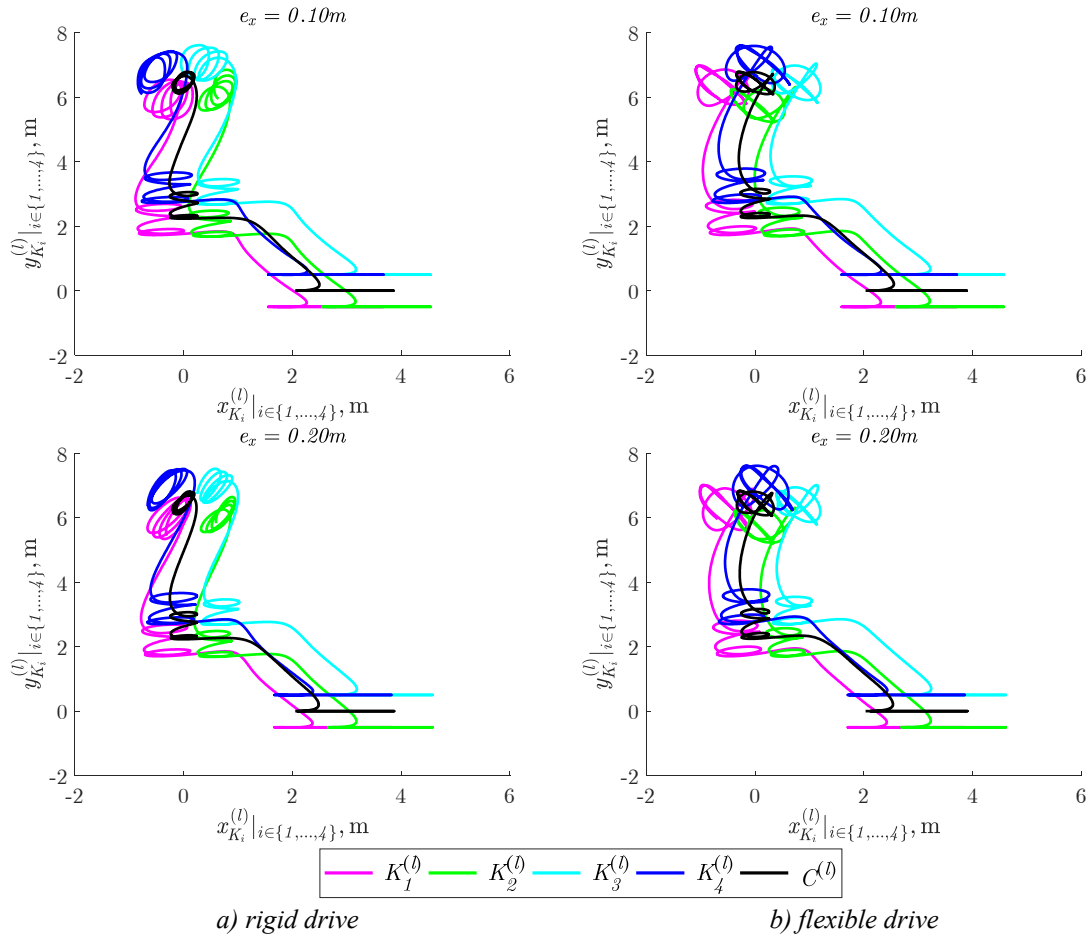

Figure 5. *Trajectories of* $K_i^{(l)}\big|_{i\in\{1,\ldots,4\}}$ *points in of the load eccentrically hanged in* $\tilde{\mathbf{x}}^{(l)}$ *axis direction*

Fig. 6 presents the trajectories of $K_i^{(l)}\big|_{i\in\{1,\ldots,4\}}$ points of the block load in $\mathbf{x}^{(0)}\mathbf{y}^{(0)}$ plane when the load is hanged eccentrically along $\tilde{\mathbf{y}}^{(l)}$ axis direction. The eccentricity is assumed as $e_y = 0.1 \text{ or } 0.2\,\text{m}$.

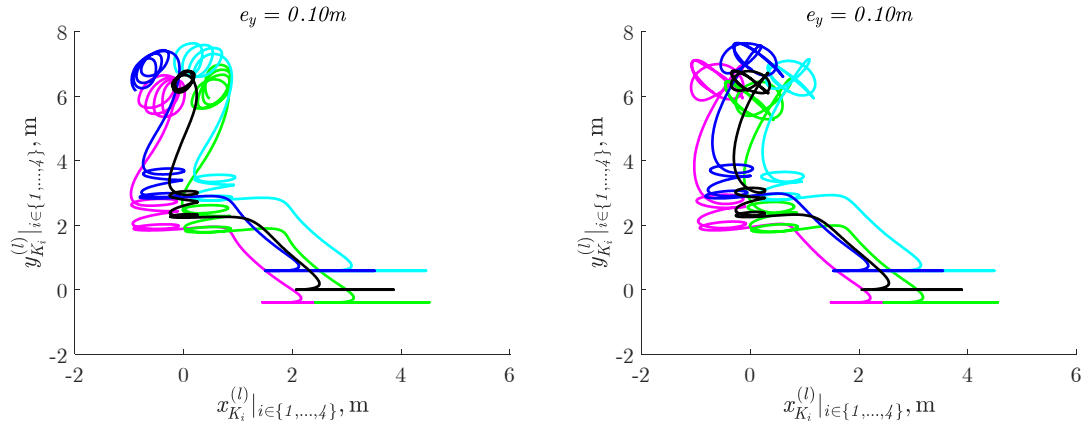

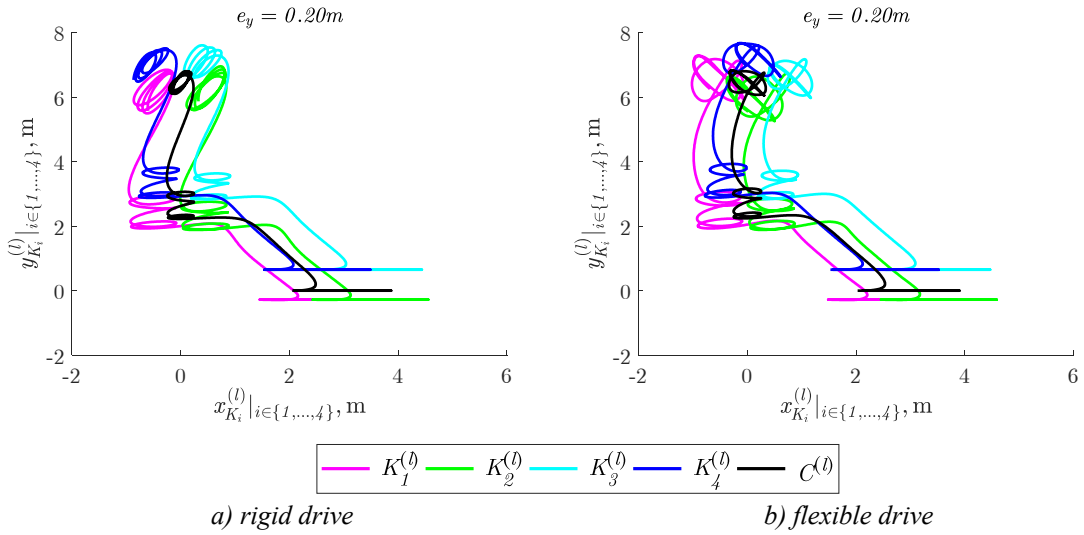

a) rigid drive *b) flexible drive*

Figure 6. *Trajectories of* $K_i^{(l)}\big|_{i\in\{1,\ldots,4\}}$ *points of the load eccentrically hanged in* $\tilde{\mathbf{y}}^{(l)}$ *axis direction*

Fig. 7 presents the trajectories of $K_i^{(l)}\big|_{i\in\{1,\ldots,4\}}$ points of the block load in the $\mathbf{x}^{(0)}\mathbf{y}^{(0)}$ plane when the load is hanged eccentrically along the bisector of the angle between $\tilde{\mathbf{x}}^{(l)}$ and $\tilde{\mathbf{y}}^{(l)}$ axes. The eccentricity is assumed as $e_{xy} = 0.1$ or $0.2\,\mathrm{m}$.

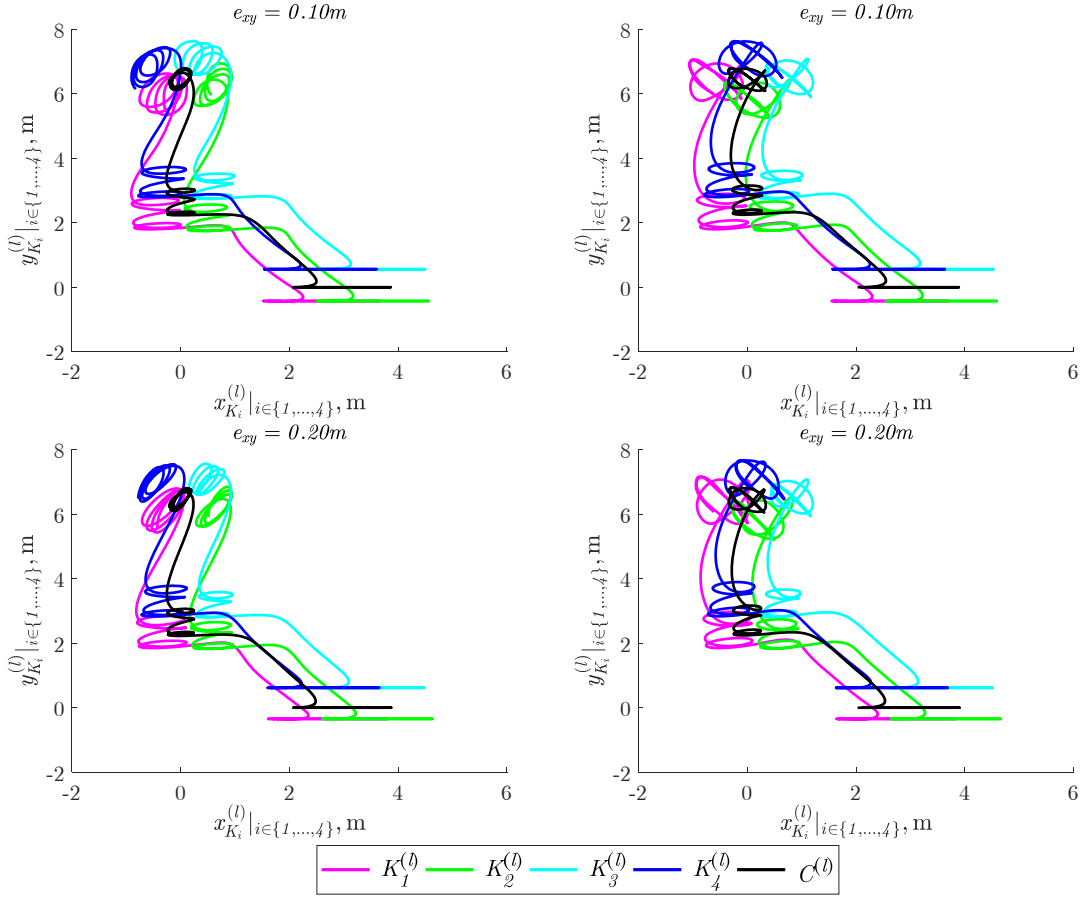

a) rigid drive *b) flexible drive*

Figure 7. *Trajectories of* $K_i^{(l)}\big|_{i\in\{1,\ldots,4\}}$ *points of the load eccentrically hanged along the bisector of the angle between* $\tilde{\mathbf{x}}^{(l)}$ *and* $\tilde{\mathbf{y}}^{(l)}$ *axes.*

In order to evaluate the influence of load hanging eccentricity, the authors propose the following indicators:

- the positioning indicator of the load during the phase of its free swings determined in relation to the centre of gravity explained in Fig. 8:

$$d_C^{(l)} = \sqrt{\left(x_{C,max}^{(l)} - x_{C,min}^{(l)}\right)^2 + \left(y_{C,max}^{(l)} - y_{C,min}^{(l)}\right)^2}, \tag{3.1}$$

where: $x_{C,max}^{(l)} = \max\left(\mathbf{x}_C^{(l)}\right)$, $x_{C,min}^{(l)} = \min\left(\mathbf{x}_C^{(l)}\right)$, $y_{C,max}^{(l)} = \max\left(\mathbf{y}_C^{(l)}\right)$, $y_{C,min}^{(l)} = \min\left(\mathbf{y}_C^{(l)}\right)$,

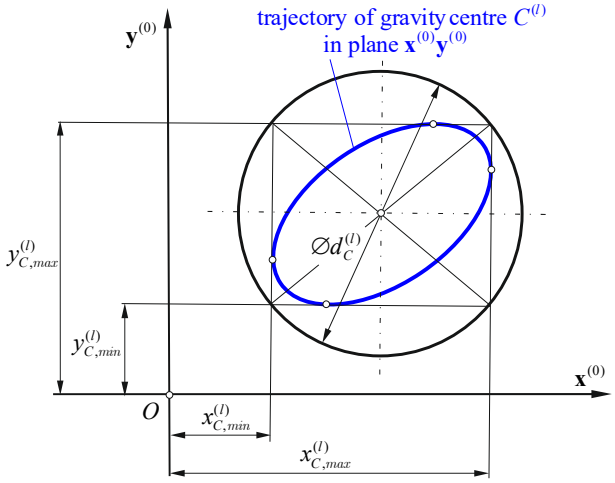

Figure 8. *Geometrical interpretation of positioning indicator $d_C^{(l)}$ of the load during the phase of its free swings*

- the positioning indicator of the load during the phase of its free swings determined in relation to $K_i^{(l)}\big|_{i\in\{1,..,4\}}$ points explained in Fig. 9:

$$d_K^{(l)} = \sqrt{\left(x_{K,max}^{(l)} - x_{K,min}^{(l)}\right)^2 + \left(y_{K,max}^{(l)} - y_{K,min}^{(l)}\right)^2}, \tag{3.2}$$

where: $x_{K,max}^{(l)} = \max\left(\mathbf{x}_{K_1}^{(l)},\ldots,\mathbf{x}_{K_4}^{(l)}\right)$, $x_{K,min}^{(l)} = \min\left(\mathbf{x}_{K_1}^{(l)},\ldots,\mathbf{x}_{K_4}^{(l)}\right)$,

$y_{K,max}^{(l)} = \max\left(\mathbf{y}_{K_1}^{(l)},\ldots,\mathbf{y}_{K_4}^{(l)}\right)$, $y_{K,min}^{(l)} = \min\left(\mathbf{y}_{K_1}^{(l)},\ldots,\mathbf{y}_{K_4}^{(l)}\right)$.

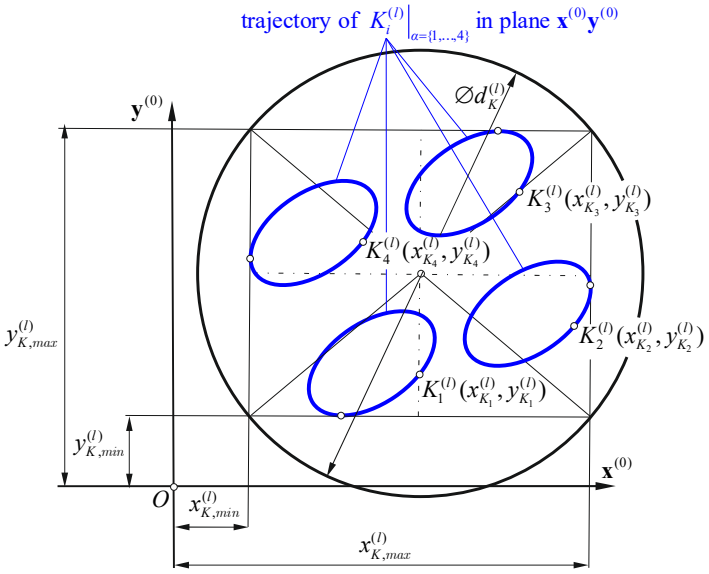

Figure 9. *Geometrical interpretation of positioning indicator $d_K^{(l)}$ of the load during the phase of its free swings*

- the positioning indicator of the load during the phase of its free swings determined in relation to $K_i^{(l)}\big|_{i\in\{1,..,4\}}$ point explained in Fig. 10:

$$h_{K_i}^{(l)}\Big|_{i=\{1,2,3,4\}} = \sqrt{\left(x_{K_i,max}^{(l)} - x_{K_i,min}^{(l)}\right)^2 + \left(y_{K_i,max}^{(l)} - y_{K_i,min}^{(l)}\right)^2}, \tag{3.3}$$

where: $y_{K_i,max}^{(l)} = \max\left(\mathbf{y}_{K_i}^{(l)}\right)$, $y_{K_i,min}^{(l)} = \min\left(\mathbf{y}_{K_i}^{(l)}\right)$, $x_{K_i,max}^{(l)} = \max\left(\mathbf{x}_{K_i}^{(l)}\right)$, $x_{K_i,min}^{(l)} = \min\left(\mathbf{x}_{K_i}^{(l)}\right)$.

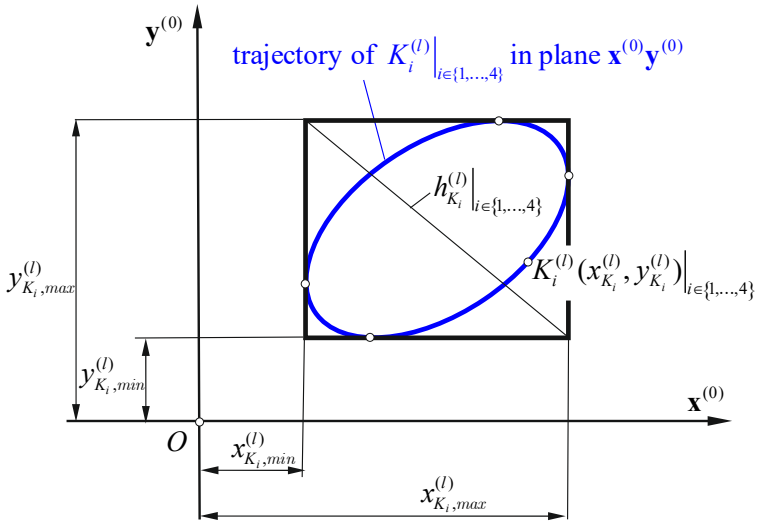

Figure 10. *Geometrical interpretation of positioning indicator* $h_{K_i}^{(l)}\big|_{i\in\{1,..,4\}}$ *of the load during the phase of its free swings*

Figs 11-13 present the numerical values of the positioning indicators defined by Eq. 3.1, 3.2, and 3.3.

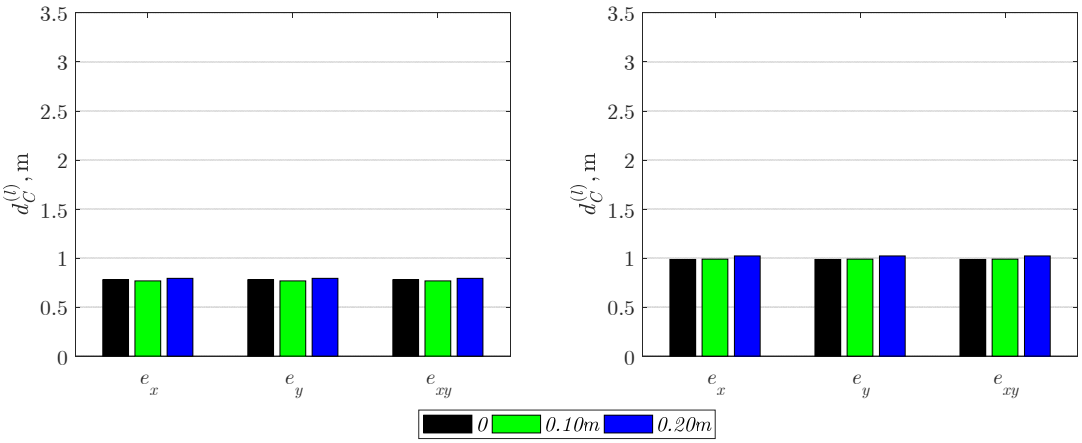

a) rigid drive *b) flexible drive*

Figure 11. *Numerical values of positioning indicator* $d_C^{(l)}$ *(Fig.7)*

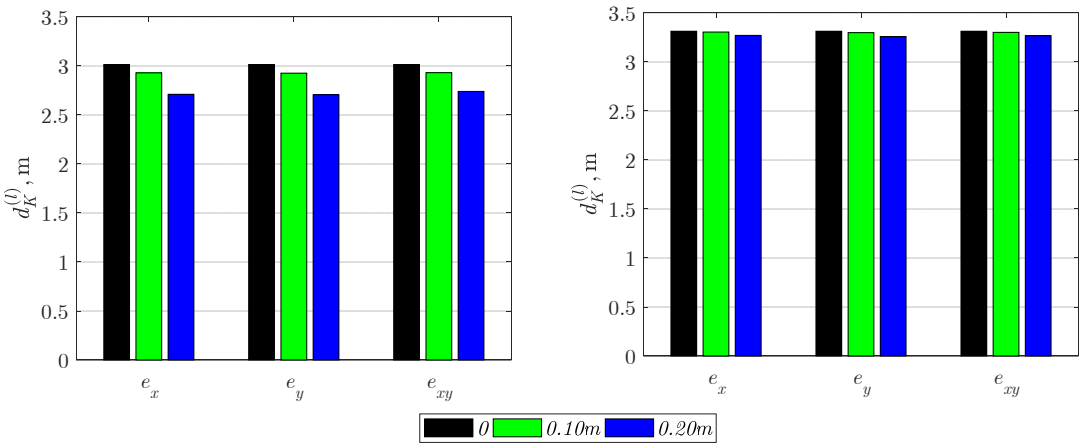

a) rigid drive *b) flexible drive*

Figure 12. *Numerical values of positioning indicator* $d_K^{(l)}$ *(Fig.8)*

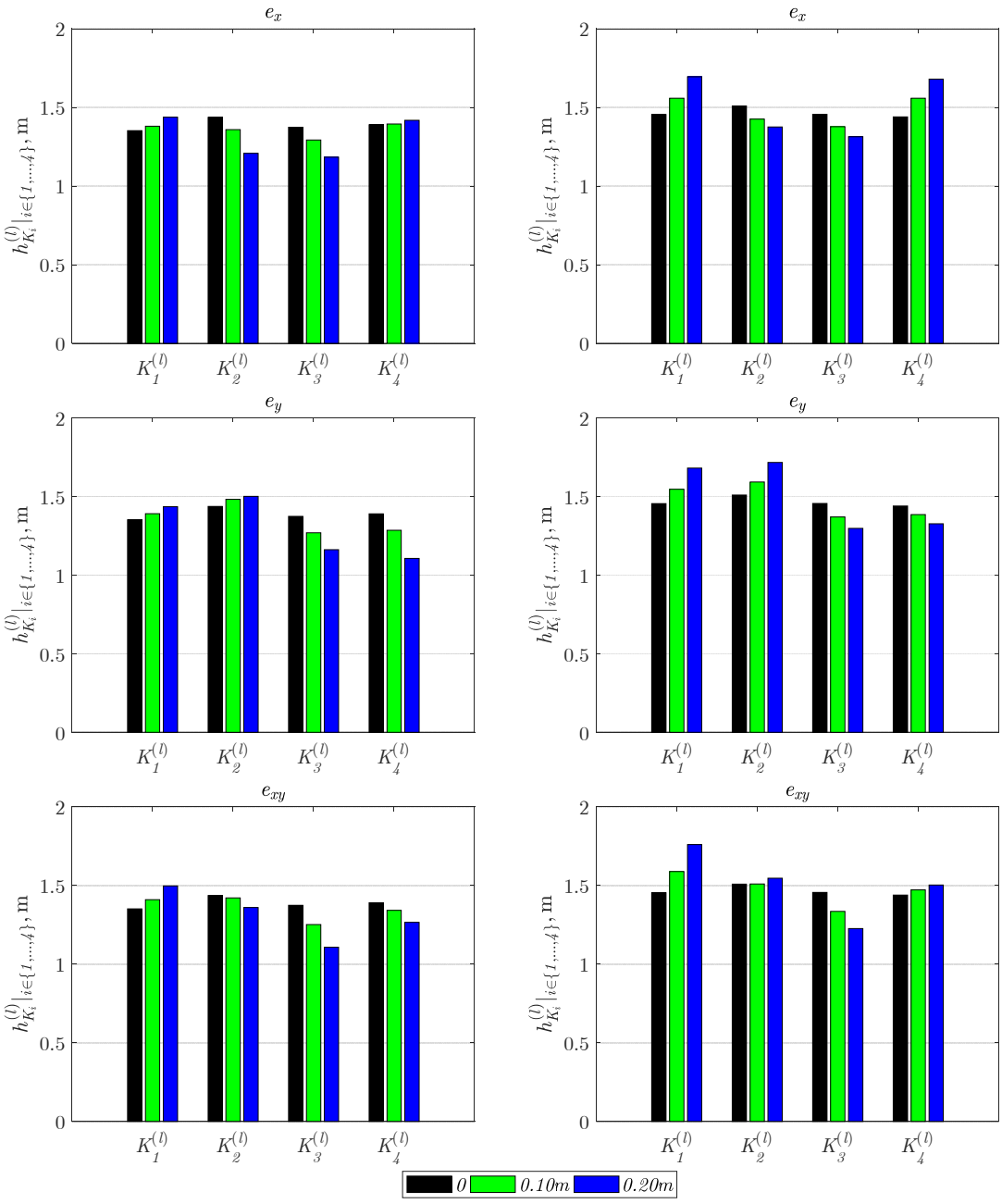

a) rigid drive *b) flexible drive*

Figure 13. *Numerical values of positioning indicator* $h_{K_i}^{(l)}\Big|_{i\in\{1,..,4\}}$ *(Fig.9)*

Analysing the obtained results, the following conclusions can be drawn:

- ✓ the method of the load and the sling modelling have significant influence on the crane's dynamics
- ✓ analysis of the trajectory of the load centre of mass is not sufficient to assess the positioning accuracy (Fig.10),
- ✓ adequate to reality assessment of load positioning accuracy in the free swings phase requires analysis of the trajectory of load characteristic points (Fig.11 and 12),
- ✓ $h_{K_i}^{(l)}\Big|_{i\in\{1,\ldots,4\}}$ indicator, which is calculated for each characteristic point (Fig.9), is the most relevant,
- ✓ the load eccentricity deteriorates the positioning accuracy, especially if the flexibility of the drives is taken into account (Fig. 10-12),
- ✓ the greatest impact of the eccentricity of the load suspension on the positioning accuracy is observed at points $K_1^{(l)}$ and $K_3^{(l)}$ (Fig.1), which coincide with the direction of the assumed eccentricity.

4 Summary

The paper analyse the influence of the load eccentricity on the load dynamics. The crane model is formulated using the Lagrange equations of the second kind. The model takes into account the eccentricity caused by the displacement of the rope sling system relative to the centroid of the load. The results obtained show analysis of the trajectory of the centre of mass of the load is insufficient, and it is more important to track the trajectory of characteristic points related to the load.

REFERENCES

[1] Gao, T., Huang, J., Singhose, W.: Eccentric-load dynamics and oscillation control of industrial cranes transporting heterogeneous loads. Mechanism and Machine Theory, 172, 104800, (2022).

[2] J. Ye, J. Huang, Analytical analysis and oscillation control of payload twisting dynamics in a tower crane carrying a slender payload, Mech. Syst. Signal Process. 158 (2021), 107763.

[3] J. Huang, X. Xie, Z. Liang, Control of bridge cranes with distributed-mass payload dynamics, IEEE/ASME Trans. Mechatron. 20 (1) (2015) 481–486.

[4] J. Huang, Z. Liang, Q. Zang, Dynamics and swing control of double-pendulum bridge cranes with distributed-mass beams, Mech. Syst. Signal Process. 54-55 (2015) 357–366.

[5] J. Peng, J. Huang, W. Singhose, Payload twisting dynamics and oscillation suppression of tower cranes during slewing motions, Nonlinear Dyn. 98 (2) (2019) 1041–1048.

[6] R. Manning, J. Clement, D. Kim, W. Singhose, Dynamics and control of bridge cranes transporting distributed-mass payloads, ASME J. Dyn. Syst. Meas. Control 132 (1) (2010), 014505.

[7] Kacalak, W., Budniak, Z., Majewski, M.: Modelling and analysis of the positioning accuracy in the loading systems of mobile cranes. Materials, 15:8426, (2022).

[8] Urbaś, A., Augustynek, K., Stadnicki, J.: Kinetic energy-based indicators to compare different load models of a mobile crane. Materials, 15:8156, (2022).